

**Manuscript version: Author's Accepted Manuscript**

The version presented in WRAP is the author's accepted manuscript and may differ from the published version or Version of Record.

**Persistent WRAP URL:**

<http://wrap.warwick.ac.uk/127763>

**How to cite:**

Please refer to published version for the most recent bibliographic citation information. If a published version is known of, the repository item page linked to above, will contain details on accessing it.

**Copyright and reuse:**

The Warwick Research Archive Portal (WRAP) makes this work by researchers of the University of Warwick available open access under the following conditions.

Copyright © and all moral rights to the version of the paper presented here belong to the individual author(s) and/or other copyright owners. To the extent reasonable and practicable the material made available in WRAP has been checked for eligibility before being made available.

Copies of full items can be used for personal research or study, educational, or not-for-profit purposes without prior permission or charge. Provided that the authors, title and full bibliographic details are credited, a hyperlink and/or URL is given for the original metadata page and the content is not changed in any way.

**Publisher's statement:**

Please refer to the repository item page, publisher's statement section, for further information.

For more information, please contact the WRAP Team at: [wrap@warwick.ac.uk](mailto:wrap@warwick.ac.uk).

# 1 **Rate dependency and Stress Relaxation of Unsaturated Clays**

2 **Meghdad Bagheri<sup>1</sup>, Mohammad Rezania<sup>2</sup>, Mohaddeseh Mousavi Nezhad<sup>3</sup>**

## 3 **Abstract**

4 This paper presents the experimental program conducted for evaluation of the rate-dependent  
5 and stress-relaxation behaviour of unsaturated reconstituted London Clay. A series of drained  
6 constant rate of strain (CRS) compression-relaxation tests with single-staged (SS-CRS) and  
7 multi-staged (MS-CRS) loading modes were performed in an innovative CRS oedometer cell  
8 where soil suction evolutions were monitored using two high-capacity tensiometers (HCTs).  
9 Specimens were tested at two strain rates of  $4.8 \times 10^{-7}$  and  $2.4 \times 10^{-6} \text{ s}^{-1}$  and over a suction range  
10 of 0 – 1905 kPa. The coupled and independent effects of strain-rate and soil suction on one-  
11 dimensional stress–strain and stress-relaxation responses including the effects of pre-relaxation  
12 strain, stress, and strain-rate under both saturated and unsaturated conditions were evaluated.  
13 An increase in suction and strain-rate resulted in an increase of the yield vertical net stress ( $\sigma_p$ ).  
14 Furthermore, it was observed that the rate and magnitude of the relaxed stresses increase with  
15 increase in pre-relaxation strain, stress, and strain-rate, and decrease with increase in soil  
16 suction. At constant suction, an increase in the pre-relaxation strain-rate by a factor of 5 resulted  
17 in an increase of the relaxed stresses by a factor of 2.2 – 3.6. Moreover, the coefficient of

---

<sup>1</sup>Lecturer, School of Energy, Construction and Environment, Coventry University, Coventry, UK.  
Email: [ac6031@coventry.ac.uk](mailto:ac6031@coventry.ac.uk). ORCID: <https://orcid.org/0000-0002-9748-4165>

<sup>2</sup>Associate Professor, School of Engineering, University of Warwick, Coventry, UK. (Corresponding Author)  
Email: [m.rezania@warwick.ac.uk](mailto:m.rezania@warwick.ac.uk). ORCID: <https://orcid.org/0000-0003-3851-2442>

<sup>3</sup>Associate Professor, School of Engineering, University of Warwick, Coventry, UK.  
Email: [m.mousavi-nezhad@warwick.ac.uk](mailto:m.mousavi-nezhad@warwick.ac.uk). ORCID: <https://orcid.org/0000-0002-0625-439X>

18 relaxation ( $R_\alpha$ ) was found to be suction-dependent, falling within a range of 0.011 – 0.019 and  
19 0.017 – 0.029 respectively for slow and fast strain rates during MS-CRS tests. Comparing these  
20 results with the  $C_d/C_c$  ratio obtained from conventional multi-stage loading (MSL) oedometer  
21 test results revealed the validity of  $R_\alpha = C_d/C_c$  correlation for unsaturated reconstituted  
22 specimens.

23 **Author Keywords:** Stress-relaxation, Strain-rate, Suction, Unsaturated soils

## 24 **Introduction**

25 The hydro-mechanical behaviour of natural clays is highly influenced by time and rate effects  
26 (Bagheri et al. 2015). The time- and rate-dependent soil parameters are the key factors for  
27 design, analysis, and construction of geotechnical structures. The effect of strain-rate is  
28 highlighted in staged construction of geo-structures where each stage of the construction plan  
29 alters the rate of soil straining in the ground. Furthermore, the construction plans often involve  
30 stages of constant total strain in the soil body during which the effective stress decreases  
31 continuously with time at a very slow rate, a phenomenon known as stress-relaxation. For  
32 instance, the soil behind supported walls of an excavation may exhibit stress-relaxation as the  
33 soil straining is restricted. Moreover, clay deposits subjected to prolonged sustained loading  
34 exhibit significant deformations with time, a phenomenon known as creep. In recent years  
35 significant attention has been given to characterisation of rate-dependency, creep, and stress-  
36 relaxation of saturated clays (e.g. Kim and Leroueil 2001; Yin and Hicher 2008; Karstunen et  
37 al., 2010; Sorensen et al., 2010; Tong and Yin, 2013; Yin et al., 2014; Rezania et al., 2017a;  
38 Rezania et al. 2017b). However, very few studies can be found in the literature accounting for  
39 the time- and rate-dependent response of unsaturated clays, this being, in part, due to the  
40 difficulties associated with the control of several parameters (i.e. time, stress, strain, suction,  
41 etc.) in an experiment. Lai et al. (2010) studied the effect of suction on creep strain-rate and

42 magnitude of reconstituted clays from the sliding zone soils of the Qianjiangping landslide in  
43 triaxial conditions and reported a decrease in creep strains with an increase in soil suction.  
44 Nazer and Tarantino (2016) investigated the viscous response (in both creep and relaxation  
45 modes) during shearing of reconstituted Ball clay using shear box and developed an analogue  
46 model for simultaneous modelling of creep and relaxation. Wang et al. (2017) performed a set  
47 of triaxial stress-relaxation tests on unsaturated lime-treated expansive clays of Hefei Xianqiao  
48 Airport site in China, at suctions of 50 and 100 kPa, and studied the effects of pre-relaxation  
49 strain level, pre-relaxation strain-rate, and relaxation time. The authors reported that for stress  
50 levels below peak deviator stress, larger relaxed stresses were observed with increase in pre-  
51 relaxation strain. Conversely, for stresses higher than the peak strength, smaller relaxed stresses  
52 were observed for higher pre-relaxation strain levels. A clear explanation of suction effects on  
53 the stress-relaxation process was not, however, presented. According to Ladanyi and  
54 Benyamina (1995), investigation of the stress–strain–time behaviour of soils can be done more  
55 conveniently by performing stress-relaxation tests rather than conventional creep tests.  
56 However, due to the lack of a unified and widely accepted formulation for correlating stress-  
57 relaxation and strain-rate-dependency and creep parameters, stress-relaxation tests have not  
58 been widely used for determination of the time-dependent response of soft soils (Borja 1992;  
59 Yin et al. 2014).

60 This paper presents the results of constant rate of strain (CRS) compression-relaxation tests on  
61 reconstituted London Clay under saturated and unsaturated conditions. An advanced suction-  
62 and temperature-controlled CRS oedometer apparatus equipped with two high-capacity  
63 tensiometers (HCTs) for monitoring suction evolutions is used for conducting the experiments.  
64 The coupled effects of strain-rate and suction on compression characteristics is investigated.  
65 Furthermore, the effect of suction, pre-relaxation strain-rate, strain, and stress level on the

66 stress-relaxation response is evaluated from a set of single-staged and multi-staged  
67 compression-relaxation tests.

## 68 **Test Material and Apparatus**

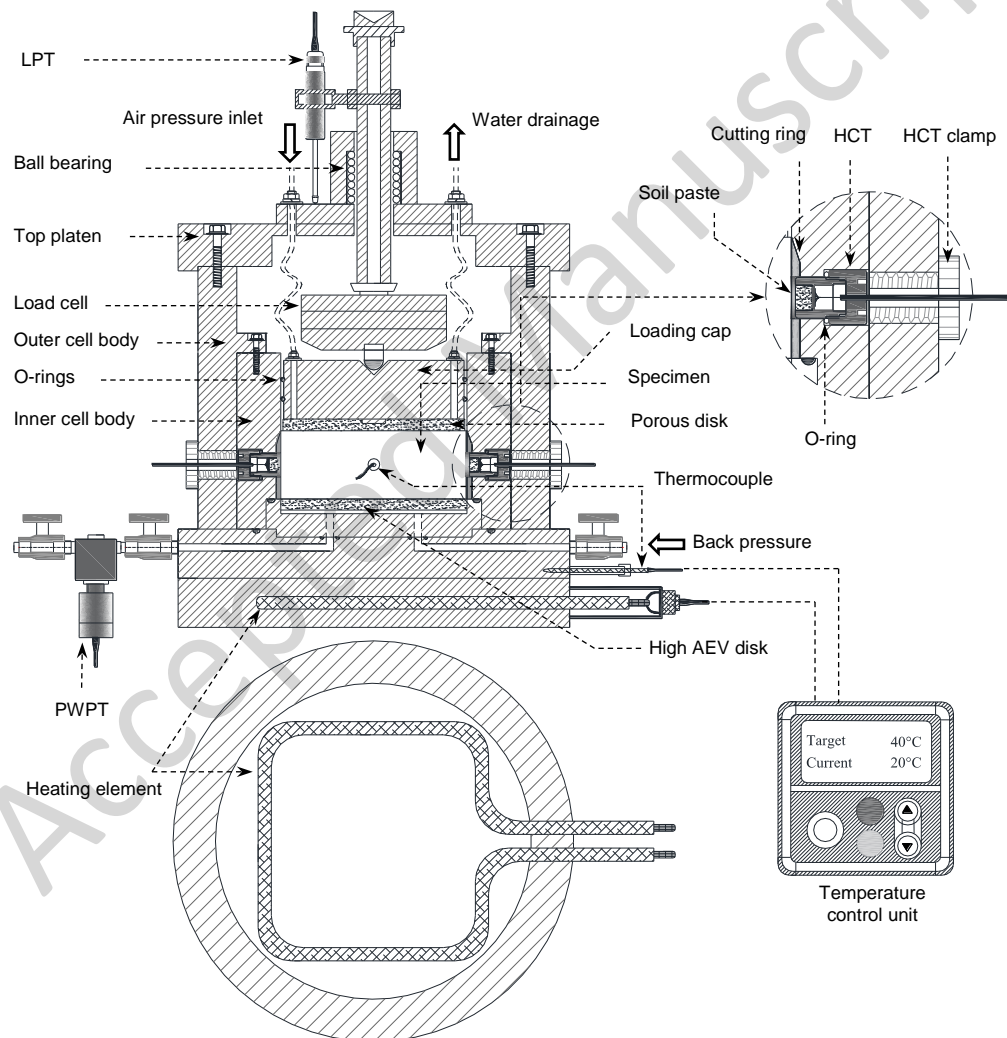
69 The material used in this study is London Clay (LC) which was collected from an engineering  
70 site in the Isle of Sheppey, UK. The natural samples were oven dried then crushed into powder  
71 and sieved through 1.18 mm opening sieve. The powder containing some course-grained peds  
72 (or large size clay clusters) was then mixed with distilled de-aired water at  $1.5w_L$ . Reconstituted  
73 samples were prepared by consolidating the soil slurry in a large diameter Perspex  
74 consolidometer. The obtained soil cake was then dried at ambient temperature to pre-specified  
75 water contents following the procedure discussed in Bagheri et al. (2019). Finally, the  
76 oedometer specimens were cored from the unsaturated samples using the cutting ring. Table 1  
77 presents the index and physical properties of the tested material. It must be noted that the  
78 presence of course-grained peds resulted in an air-entry value (AEV) of around 250 kPa  
79 (Bagheri et al. 2019) which is notably lower than the AEV of natural LC reported in the  
80 literature. The lower AEV allows for testing specimens over a wider range of soil suctions in  
81 unsaturated states. All experiments were carried out on reconstituted specimens in order to  
82 eliminate the effect of soil structure (mainly inter-particle bonding) on the test results.

83 **Table 1.** Index and physical properties of the reconstituted LC samples

Grain size, D (mm)			Index properties			
D < 0.002	0.002 < D < 0.063	D > 0.063	$w_P$	$w_L$	$I_P$	$G_s$
58%	30%	12%	18%	68%	50%	2.67

84 An advanced suction- and temperature-controlled CRS oedometer cell (see Bagheri et al. 2019)  
85 was used for conducting CRS compression and relaxation tests under saturated and unsaturated  
86 conditions. The new CRS oedometer system made it possible to perform multi-staged tests

87 which included 1D compression tests; (1) at a constant rate of strain to investigate the coupled  
88 effects of suction and strain-rate, and (2) with rest periods at intermediate stages with fixed  
89 axial strain to investigate the effects of suction, pre-relaxation strain, stress, and strain-rate on  
90 the stress-relaxation behaviour. Fig. 1 presents a schematic diagram of the apparatus. Two  
91 HCTs, accommodated at the mid-height of the specimen, allowed for continuous measurement  
92 of pore-water pressure (suction) evolutions throughout the experiments (see Bagheri et al. 2018  
93 for more information about the design characteristics of the HCTs).



94

95 **Fig. 1.** Schematic diagram of the CRS cell structure and components (Bagheri et al. 2019)

96

## 97 **Experimental Program**

98 Drained CRS compression tests were carried out on saturated and unsaturated specimens at  
99 two different strain-rates of  $\dot{\epsilon}_v = 4.8 \times 10^{-7}$  (denoted by letter A) and  $\dot{\epsilon}_v = 2.4 \times 10^{-6} \text{ s}^{-1}$  (denoted  
100 by letter B). Two types of tests were carried out; single-staged compression-relaxation tests  
101 (SS-CRS), and multi-staged compression-relaxation tests (MS-CRS). A set of 10 drained SS-  
102 CRS tests were carried out, each test comprising of two stages; (1) loading the specimen at a  
103 constant rate of displacement to a vertical total stress of  $\sigma_0 \cong 3450 \text{ kPa}$ , and (2) stress-relaxation  
104 at zero rate of axial displacement for a period of at least  $t_R \cong 210$  hours. This set of experiments  
105 allow for investigation of suction and strain-rate effects on the compression and stress-  
106 relaxation processes. Table 2 summarises the details of the compression stage of the SS-CRS  
107 tests.

108 A set of two MS-CRS tests were carried out on unsaturated specimens, having an initial suction  
109 of  $s_0 \cong 701 \text{ kPa}$  (initial water content of  $w_0 = 33\%$ ). The test procedure involved loading the  
110 specimens at a constant rate of displacement with stress-relaxation stages of 24 hours duration  
111 set at different strain levels as summarised in Table 3. This set of experiments allow for  
112 investigation of pre-relaxation strain level, stress level, and strain-rate on the stress-relaxation  
113 process. Before commencing each experiment, the preparation of the cell was carried out  
114 according to the procedure described in Bagheri et al. (2019). The HCTs were also  
115 preconditioned (see Bagheri et al. (2018) for more details). All tests were performed in a  
116 temperature-controlled laboratory environment to avoid the influence of temperature  
117 fluctuations on the output data. The maximum values of  $PPR$  (denoted by  $PPR_{max}$ ) for selected  
118 strain-rates were found to be within a range of 1 – 9%, complying well with the suggested  
119  $PPR_{max}$  range of 3 – 15% by ASTM-D4186-06 (2006).  $PPR$  is defined as the ratio of the excess  
120 pore-water pressure ( $u_{exc}$ ) to the applied vertical total stress ( $\sigma_v$ ).



121

**Table 2.** Details of the compression stage of the SS-CRS tests

Test ID	$w_0$ [%]	$s_0$ [kPa]	$\dot{\epsilon}_v$ [s <sup>-1</sup> ]	$PPR_{max}$ [%]	$\sigma_p$ [kPa]	$\sigma_0$ [kPa]
CRSrs39-A	39	0	$4.8 \times 10^{-7}$	4.9	157	3451
CRSru33-A	33	701	$4.8 \times 10^{-7}$	2.9	436	3422
CRSru32-A	32	802	$4.8 \times 10^{-7}$	9.0	539	3440
CRSru30-A	30	1045	$4.8 \times 10^{-7}$	8.0	676	3448
CRSru26-A	26	1905	$4.8 \times 10^{-7}$	1.1	1493	3459
CRSrs43-B	43	0	$2.4 \times 10^{-6}$	8.5	108	3488
CRSrs39-B	39	0	$2.4 \times 10^{-6}$	6.0	227	3451
CRSru36-B	36	433	$2.4 \times 10^{-6}$	4.9	288	3445
CRSru33-B	33	701	$2.4 \times 10^{-6}$	3.4	655	3442
CRSru26-B	26	1905	$2.4 \times 10^{-6}$	1.4	1551	3444

r: reconstituted, s: saturated, u: unsaturated, A and B: strain rates  
 The number before dash indicates initial water content.

122

**Table 3.** Details of MS-CRS tests

Test ID	$w_0$ [%]	$s_0$ [kPa]	$\dot{\epsilon}_v$ [s <sup>-1</sup> ]	$\epsilon_R$ [%]
MCRSru33-A	33	701	$4.8 \times 10^{-7}$	5, 10, 15, 18
MCRSru33-B	33	701	$2.4 \times 10^{-6}$	5, 10, 15, 17

r: reconstituted, u: unsaturated, A and B: strain rates  
 The number before dash indicates initial water content.

123

The experimental results of saturated tests are evaluated based on the effective stress principle

124

( $\sigma'_v = \sigma_v - u_w$ ). Simplified methods for calculation of unsaturated effective stress based on the

125

single effective stress approach can be found in Khoshghalb and Khalili (2013) and

126

Khoshghalb et al. (2015). However, in this work, the experimental results of unsaturated tests

127

are evaluated based on the vertical net stress ( $\sigma_{vnet} = \sigma_v - u_a$ ). Since the tests were carried out at

128

the atmospheric air pressure, the vertical net stress is equal to the applied vertical total stress.

129

Where the results of saturated and unsaturated CRS tests were to be plotted on the same graph,

130

the saturated tests were also interpreted based on vertical net stress. Moreover, in order to allow

131

for comparing the results with those reported in the literature, the mechanical path is

132

represented in terms of axial strain ( $\epsilon_a$ ) and  $\sigma_{vnet}$ . The compression index ( $C_c$ ) is calculated as

133

the slope of the normal compression line (NCL) of the compression curve plotted in  $e/e_0 - \log$

134

$\sigma_{vnet}$  space, where  $e/e_0$  represents the void ratio ( $e$ ) normalised with respect to the initial void



135 ratio ( $e_0$ ). The yield vertical net stress ( $\sigma_p$ ) is determined as the intersection of the best fitted  
136 lines to the pseudo-elastic and plastic sections of the compression curve. The stress-relaxation  
137 process is evaluated using three main parameters; the coefficient of relaxation ( $R_\alpha$ ), the residual  
138 stress ratio ( $\xi$ ), and the relaxed stress ( $\Delta\sigma$ ).  $R_\alpha$  is defined as the slope of the plot of  $\sigma_{vnet}$  versus  
139 time ( $t$ ) in  $\log \sigma_{vnet} - \log t$  space during relaxation of the stresses;

$$R_\alpha = -\frac{\Delta \log(\sigma_{vnet})}{\Delta \log(t)} \quad (1)$$

140 The residual stress ratio ( $\xi$ ) is defined as the ratio of the residual total vertical stress ( $\sigma_s$ ) and  
141 the pre-relaxation total vertical stress ( $\sigma_0$ ). The residual total vertical stress is the stress value  
142 at the end of the relaxation course.

$$\xi = \frac{\sigma_s}{\sigma_0} \quad (2)$$

143 The relaxed stress ( $\Delta\sigma$ ) is defined as;

$$\Delta\sigma = \sigma_0 - \sigma_s \quad (3)$$

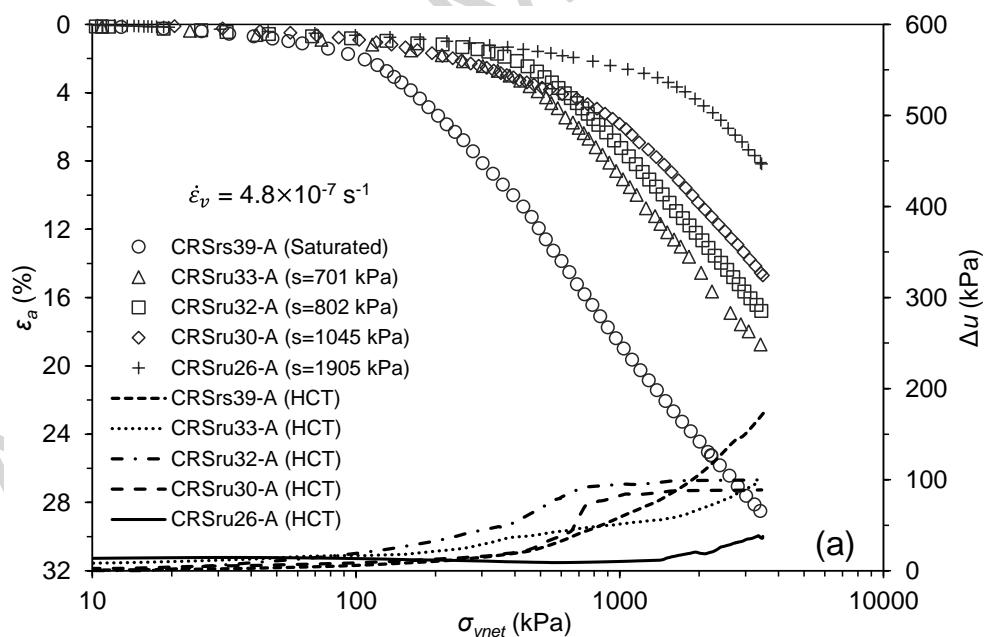
144 Similar parameters were introduced by Wang et al. (2017) for interpretation of the stress-  
145 relaxation process in triaxial conditions.

## 146 **Discussion of the Results**

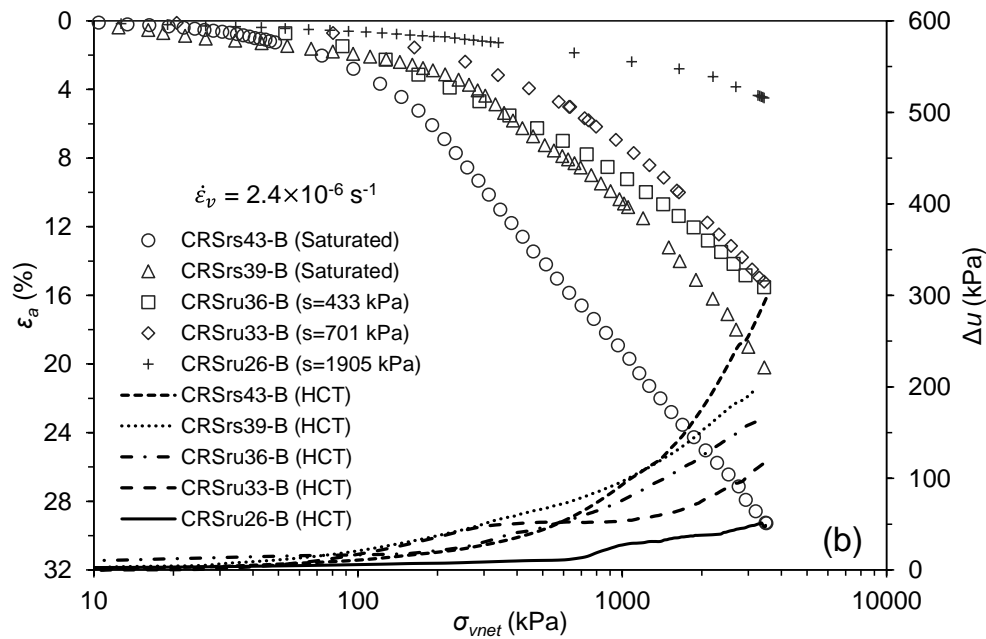
### 147 ***Effect of Suction and Strain-rate on Stress-Relaxation Response***

148 Fig. 2 illustrates the results of the compression stage of the SS-CRS tests. Also shown in the  
149 graphs, are the change in pore-water pressure ( $\Delta u = u_w - u_{exc}$ ) with  $\sigma_{vnet}$ . As the pore-water  
150 pressure (suction) measurements recorded by the two HCTs installed on each specimen were  
151 very similar, only measurements from one of the HCTs are presented in the graphs.

152 Inspection of the results reveals the suction-dependency of the stress–strain behaviour during  
 153 1D compression. As can be seen, the overall compressibility of the specimens decreases with  
 154 increase in suction and strain-rate. Moreover, increase in suction resulted in an increase in  $\sigma_p$   
 155 values for both sets of experiments carried out at different strain-rates. The values of  $\sigma_p$  vary  
 156 with strain-rates at the strain level of 2 – 3%. Slope of the normal consolidation lines (NCLs)  
 157 for both sets of tests were found to be suction-dependent and decrease with increase in suction,  
 158 within the range of applied vertical stresses. This effect was more pronounced for higher strain-  
 159 rate tests. Furthermore, by extrapolating the compression curves to higher stress levels (i.e.  
 160 greater than 3.5 MPa), it is anticipated that the slope of NCLs will eventually converge at a  
 161 constant value corresponding to that of saturated specimen, as suggested by Zhou et al. (2012).  
 162 Inspecting the variation of  $u_{exc}$  with  $\sigma_{vnet}$  reveals that the higher the strain-rate, the higher the  
 163 generated  $u_{exc}$ . The rate of change of  $\Delta u$  was also found to decrease with increase in suction.



164

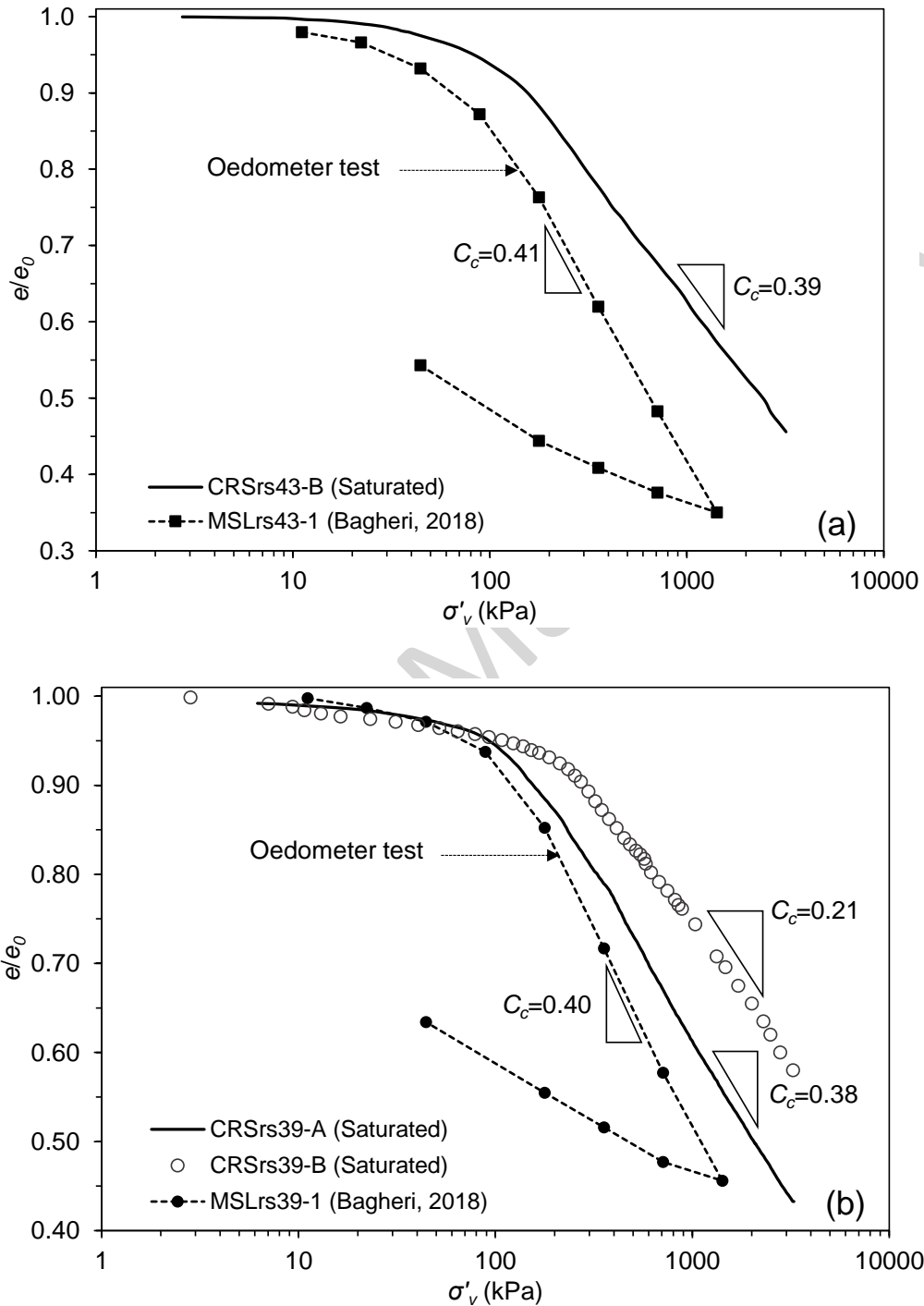


165

166 **Fig. 2.** CRS compression curves at different suction levels for strain-rates of: (a)  $4.8 \times 10^{-7} \text{ s}^{-1}$ ; (b)  
 167  $2.4 \times 10^{-6} \text{ s}^{-1}$

168 Fig. 3 presents a comparison of the compression curves obtained from CRS test and the  
 169 conventional multi-staged loading (MSL) oedometer tests (Bagheri 2018) for saturated  
 170 specimens (prepared with similar procedure) with  $w_0$  of 43 and 39%. It is observed that the  
 171 compression curves from CRS tests are shifted to the right, exhibiting higher preconsolidation  
 172 pressure than the MSL tests. Moreover, the figure shows that at a given void ratio, the higher  
 173 the strain-rate the higher the vertical effective stress. The strain-rate values chosen for the CRS  
 174 tests are generally higher than the observed strain-rates during creep phases of conventional  
 175 oedometer tests. This results in the CRS compression curves lying above the MSL compression  
 176 curves. Selection of very slow strain-rates, in addition to significantly increasing testing time,  
 177 can give rise to aging effects and gradual development of inter-particle bonding, which leads  
 178 to an increase in  $\sigma_p$  and shift of the CRS compression curve to the right (Leroueil et al. 1996;  
 179 Qiao et al. 2016). This is also the case when a specimen, subjected to prolonged creep at very  
 180 low strain-rates, is loaded (Sorensen et al. 2010). A CRS compression curve with a very slow

181 strain-rate may also lie above a CRS compression curve with much faster strain-rate, due to the  
 182 aging effects.



183

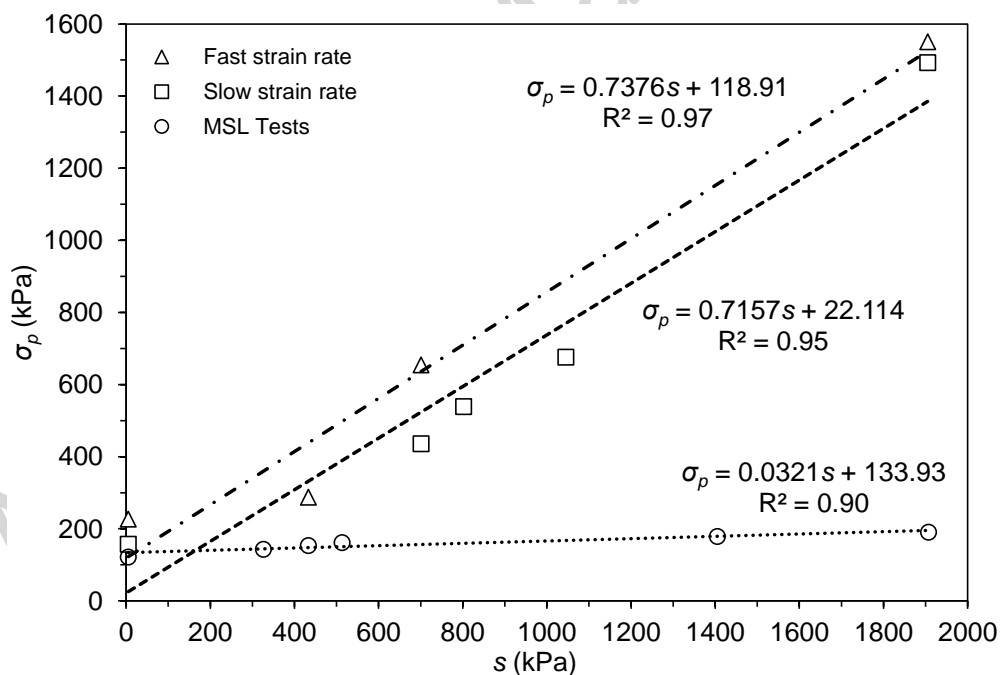
184

185 **Fig. 3.** Comparison of compression curves obtained from CRS and MSL tests on saturated specimens

186

with initial water contents of: (a) 43%; (b) 39%

187 Fig. 4 presents the variation of  $\sigma_p$  with suction for both MSL and CRS tests. It is observed that  
 188 at a constant suction, the higher the strain-rate, the higher the  $\sigma_p$ . Similarly, at a constant strain-  
 189 rate, the higher the suction, the higher the  $\sigma_p$ . Additionally, the increase in  $\sigma_p$  with suction  
 190 appears to follow an approximately linear trend for fast, slow, and oedometric strain-rates. An  
 191 average value of 1.3 has been reported in the literature for the ratio of  $\sigma_p$  obtained from CRS  
 192 and MSL tests ( $\sigma_{pCRS}/\sigma_{pMSL}$ ) on saturated soft clays for strain-rates in a range of  $1 \times 10^{-6}$  to  $4 \times 10^{-6}$   
 193  $s^{-1}$  (Leroueil et al. 1983; Hanzawa et al. 1990; Nash et al. 1992; Cheng and Yin 2005). The  
 194  $\sigma_{pCRS}/\sigma_{pMSL}$  ratio for specimens with  $w_0 = 0.39$  (saturated) is calculated as 1.29 which is very  
 195 close to the average value reported for soft clays in abovementioned studies. This ratio can  
 196 therefore be considered as a function of the loading mode rather than the sample type (i.e.,  
 197 intact or reconstituted).



198  
 199 **Fig. 4.** Variation of  $\sigma_p$  with suction for fast, slow, and oedometric strain-rates.

200 As mentioned earlier, the stress-relaxation process was initiated right after the test specimens,  
 201 loaded at different strain-rates of A and B, reached a maximum vertical stress of approximately  
 202 3450 kPa. The gradual decrease of stresses with time were recorded and used for evaluation of

203 the effects of pre-relaxation strain-rate, relaxation time ( $t_R$ ), and suction, on the stress-  
 204 relaxation process. Monitoring suction evolutions during the course of stress-relaxation for  
 205 CRSru26-A and CRSru26-B, having initial suctions of approximately 1905 kPa, was  
 206 interrupted due to the cavitation of the HCTs. Due to the sensitivity of the stress-relaxation  
 207 stage, no attempt was made to replace the cavitated HCTs, and hence, the suction  
 208 measurements are not available for these two experiments. The final values of soil suction  
 209 were, however, measured at the end of the tests. Table 4 summarises the characterisation  
 210 parameters. In order to provide a platform for comparison, the values of  $\sigma_s$  corresponding to  $t_R$   
 211 = 210 hours are used for calculation of the relaxation parameters  $\Delta\sigma$ ,  $\zeta$ , and  $R_a$ .

212 **Table 4.** Characterisation parameters for stress-relaxation stage of the SS-CRS tests

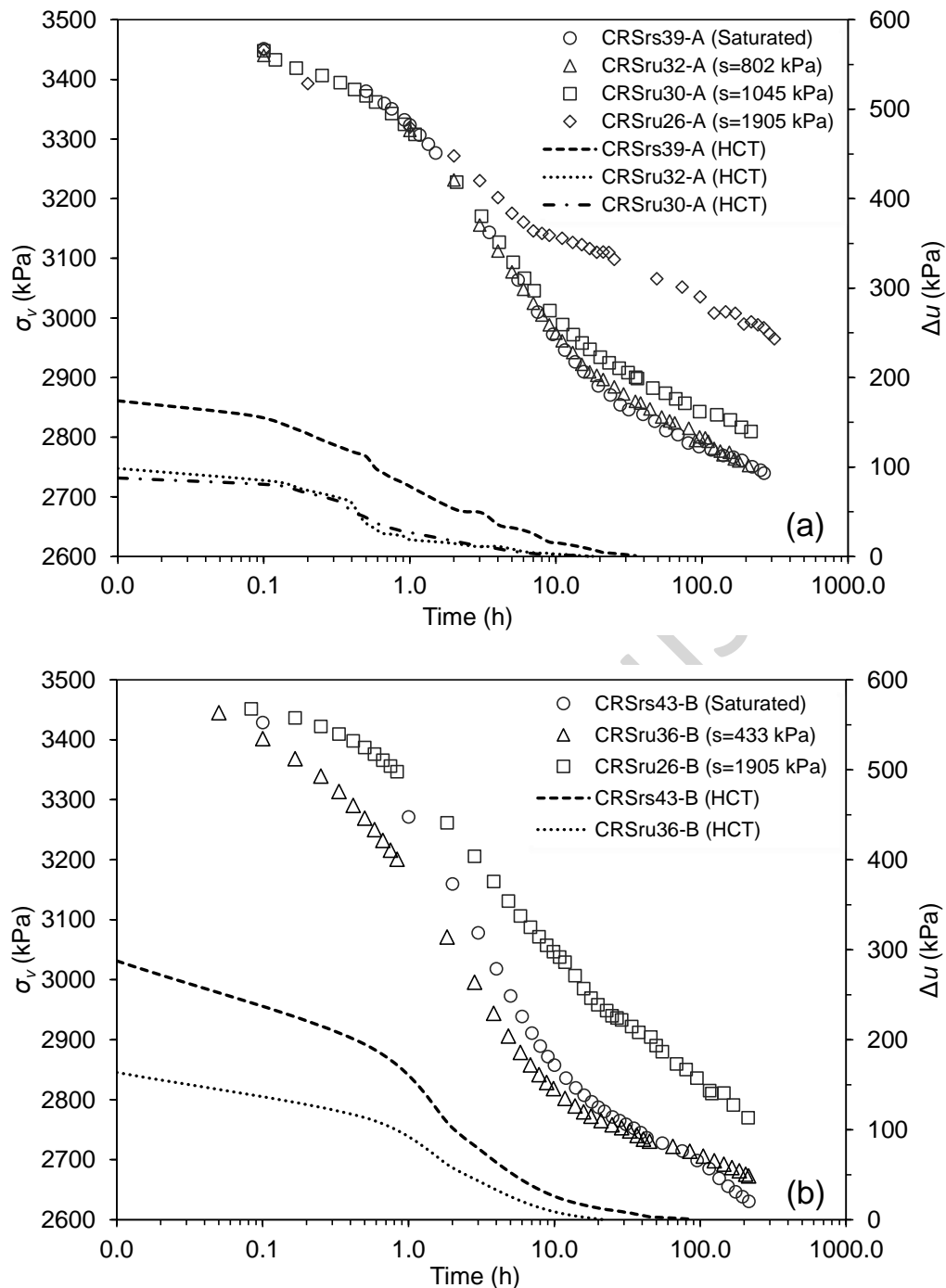
Test ID	$s_0$ [kPa]	$\dot{\epsilon}_v$ [s <sup>-1</sup> ]	$\sigma_0$ [kPa]	$\sigma_s$ [kPa]	$\Delta\sigma$ [kPa]	$\Delta\sigma/\sigma_0$ [%]	$\zeta$	$R_a$	$t_R$ [h]
CRSrs39-A	0	$4.8 \times 10^{-7}$	3451	2743	711	21	0.79	0.019	266
CRSru32-A	802	$4.8 \times 10^{-7}$	3440	2752	688	20	0.80	0.019	210
CRSru30-A	1045	$4.8 \times 10^{-7}$	3448	2809	639	19	0.81	0.018	216
CRSru26-A	1905	$4.8 \times 10^{-7}$	3459	2989	494	14	0.86	0.011	313
CRSrs43-B	0	$2.4 \times 10^{-6}$	3435	2630	805	23	0.77	0.029	215
CRSru36-B	433	$2.4 \times 10^{-6}$	3445	2674	771	22	0.78	0.017	215
CRSru26-B	1905	$2.4 \times 10^{-6}$	3452	2823	629	18	0.82	0.017	213

213 Considering the values of relaxation parameters given in Table 4, it is found that, at constant  
 214 pre-relaxation stress ( $\sigma_0$ ), increase in suction resulted in a decrease of the relaxed stresses ( $\Delta\sigma$ )  
 215 and consequently an increase of the stress-relaxation ratio ( $\zeta$ ). In other words, with increase in  
 216 suction from 0 to 1905 kPa, the ratio  $\Delta\sigma/\sigma_0$  was reduced from 21 to 14% for specimens loaded  
 217 at the slow strain-rate (A), and from 23 to 18% for specimens loaded at the fast strain-rate (B).  
 218 Effect of suction in reduction of relaxed stresses appears to be reasonable, considering the  
 219 stress-relaxation mechanism as a time-dependent process of particles re-adjustment and  
 220 gradual change in the structural configuration of grains. In essence, the additional bonding  
 221 forces exerted by the under-tension water menisci developed at the inter-particle contacts, can

222 prevent re-arrangement of particles, and hence, release of stresses accumulated during the  
223 loading stage.

224 Fig. 5 presents the relaxation of vertical stress with time in a semi-log plot. Also shown in the  
225 graphs, are the plots of dissipation of  $u_{exc}$  with time during the stress-relaxation stage. The  
226 process of stress-relaxation appears to involve three phases of; (1) fast relaxation, (2)  
227 decelerating relaxation, and (3) residual relaxation as schematically shown in Fig. 6. The fast  
228 relaxation phase is associated with a quick release of the main accumulated energy inside the  
229 specimen, whereas the deceleration and residual phases correspond to the time-dependent  
230 particles re-arrangement which involves further dissipation of energy with time. At a constant  
231 strain-rate, suction appears to have more influence on the stress-relaxation process during fast  
232 and deceleration phases. In fact, the higher the suction, the lower would be the rate of relaxation  
233 during fast and decelerating relaxation phases. Similarly, at a constant suction, the higher the  
234 pre-relaxation strain-rate, the higher would be the rate and magnitude of the relaxed stresses as  
235 shown in Fig. 7 for CRSru26-A and CRSru26-B specimens (see also Table 4 for corresponding  
236 relaxation parameters). Similar observations were reported by Wang et al. (2017) from the  
237 results of triaxial stress-relaxation tests on unsaturated lime-treated expansive clay specimens.





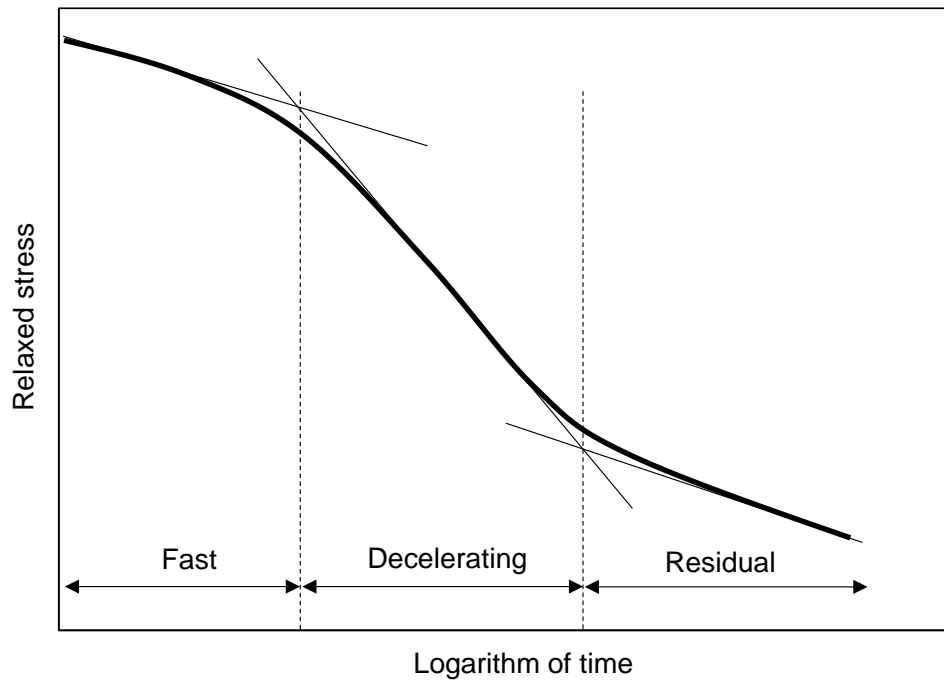
238

239

240 **Fig. 5.** Stress-relaxation and associated excess pore-water pressure dissipation in SS-CRS oedometer  
 241 tests at: (a)  $4.8 \times 10^{-7} \text{ s}^{-1}$ ; (b)  $2.4 \times 10^{-6} \text{ s}^{-1}$

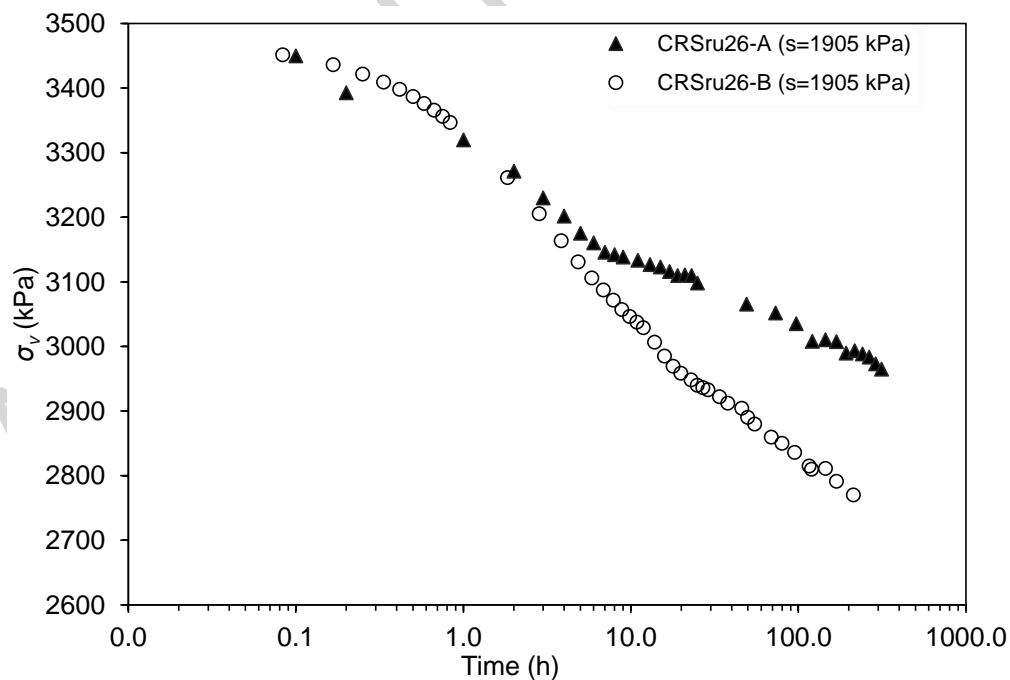
242 It must be noted that, except for the saturated specimens where a slight drainage of water was  
 243 observed, the processes of  $u_{exc}$  dissipation did not involve any significant volume change, given  
 244 the preservation of suction state in the unsaturated specimens. Effect of pore-water pressure

245 dissipation during relaxation stage of 1D CRS tests on saturated reconstituted LC was also  
246 reported by Sorensen (2006).



247  
248

**Fig. 6.** Stress-relaxation phases

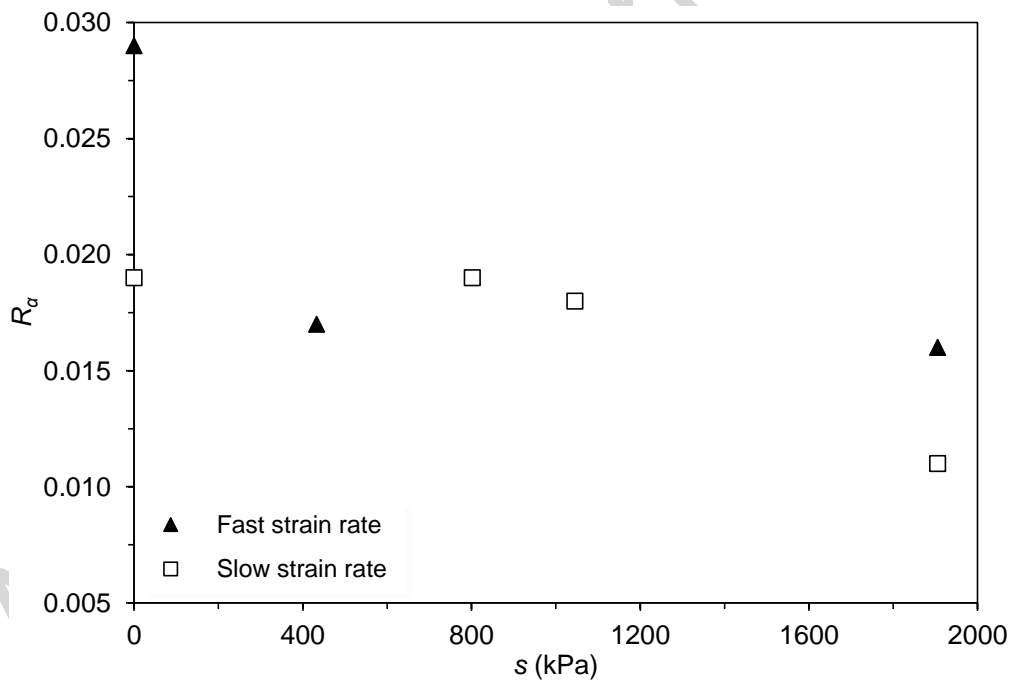


249  
250

**Fig. 7.** Effect of strain-rate on the stress-relaxation response

251 Fig. 8 presents the variation of relaxation coefficient ( $R_a$ ) with suction for fast and slow strain-  
252 rates. Although there is a clear difference between the  $R_a$  values corresponding to saturated ( $s$

253 = 0) and unsaturated (e.g.  $s = 1905$  kPa) states, with the limited number of data points, it is  
254 hard to comment on the relationship between  $R_\alpha$  and suction. For the slow and fast strain-rates,  
255 the values of  $R_\alpha$  fall within a range of 0.011 – 0.019 and 0.017 – 0.029 respectively. As  
256 suggested by Yin et al. (2014), the values of  $R_\alpha$  are equal to the values of  $\alpha = C_\alpha/C_c$  ratio and  
257 can be used for estimation of creep index ( $C_\alpha$ ) and compression index ( $C_c$ ). Bagheri (2018)  
258 showed that the values of  $\alpha$  were also suction- and stress-dependent and fall within a range of  
259 0.023 – 0.030 for MSL tests on unsaturated reconstituted LC specimens. This range, with a  
260 good approximation, complies with the  $R_\alpha$  range of 0.017 – 0.029 obtained from fast strain-rate  
261 tests, hence, validating the applicability of  $R_\alpha = \alpha$  for saturated and unsaturated reconstituted  
262 specimens tested in this study.



263  
264 **Fig. 8.** Variation of relaxation coefficient ( $R_\alpha$ ) with suction

### 265 ***Effect of Pre-relaxation Stress Level***

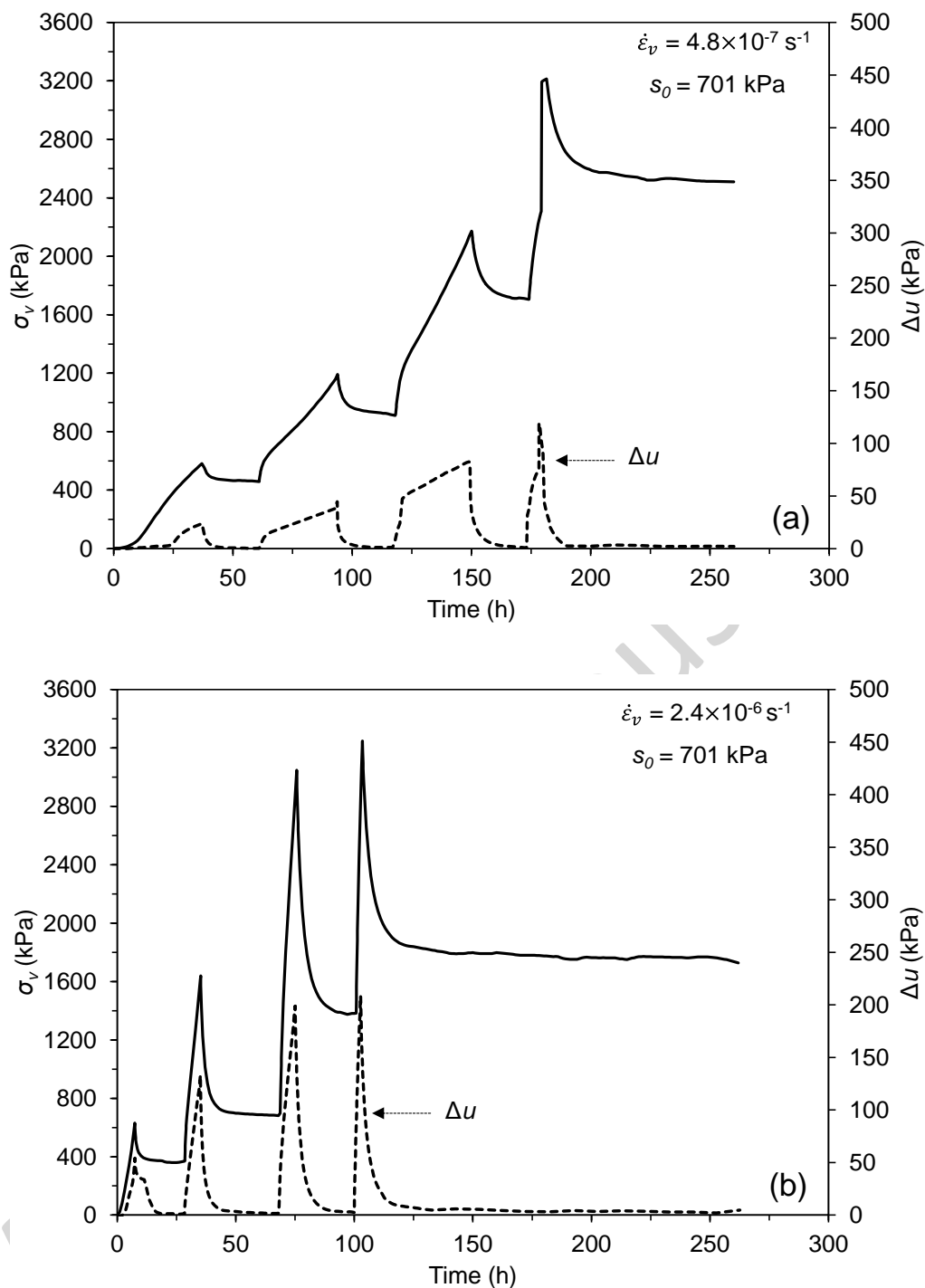
266 Fig. 9 illustrates the variations of  $\sigma_v$  with time during MS-CRS tests. Also shown in the graphs,  
267 are the change in pore-water pressure ( $\Delta u$ ) with time (dotted lines). The characterisation

268 parameters for stress-relaxation stages are summarised in Table 5. In order to provide a  
 269 platform for comparison, the values of  $\sigma_s$  corresponding to  $t_R = 24$  hours are used for calculation  
 270 of the relaxation parameters  $\Delta\sigma$ ,  $\xi$ , and  $R_\alpha$ .

271 **Table 5.** Characterisation parameters for stress-relaxation stage of the MS-CRS tests

Test ID	$\varepsilon_R$ [%]	$\sigma_0$ [kPa]	$\sigma_s$ [kPa]	$\Delta\sigma$ [kPa]	$\Delta\sigma/\sigma_0$ [%]	$\xi$	$R_\alpha$	$t_R$ [h]
MCRSru33-A	5	581	459	122	21	0.79	0.011	24
	10	1192	910	282	24	0.76	0.022	24
	15	2172	1705	467	22	0.78	0.025	24
	18	3213	2574 (2510)	639 (703)	20 (22)	0.80	0.027	24 (78)
MCRSru33-B	5	630	359	271	43	0.57	0.025	22
	10	1639	688 (682)	951 (957)	58 (58)	0.42	0.026	24 (33)
	15	3047	1381	1666	55	0.45	0.028	24
	17	3248	1833 (1731)	1415 (1517)	44 (47)	0.56	0.035	24 (452)
Values in the parentheses correspond to the values obtained at the end of the final relaxation stages.								

272 The values of relaxed stresses ( $\Delta\sigma$ ) are found to increase with increase in the pre-relaxation  
 273 strain ( $\varepsilon_R$ ) for the specimen loaded at the slow strain-rate. However, the values of  $\Delta\sigma/\sigma_0$  ratio  
 274 increase from 21 to 24% for an increase in  $\varepsilon_R$  from 5 to 10%, then decrease to 22 and 20%  
 275 respectively for pre-relaxation strains of 15 and 18%. Similarly, for the specimen loaded at the  
 276 fast strain-rate, the values of  $\Delta\sigma$  are found to increase with increase in the pre-relaxation strain  
 277 up to 15% at which it decreases to a lower value at  $\varepsilon_R = 17\%$ . The values of  $\Delta\sigma/\sigma_0$  ratio increase  
 278 from 43 to 58% for an increase in  $\varepsilon_R$  from 5 to 10%, then decrease to 55 and 44% respectively  
 279 for pre-relaxation strains of 15 and 17%. Overall, larger relaxed stresses are observed with  
 280 increase in pre-relaxation strains (and consequently pre-relaxation stresses). Moreover, an  
 281 increase in the pre-relaxation strain-rate by a factor of 5, is found to significantly affect the  
 282 magnitude of relaxed stresses at each pre-relaxation strain level, resulting in an increase of the  
 283  $\Delta\sigma$  values by a factor of 2.2 – 3.6.



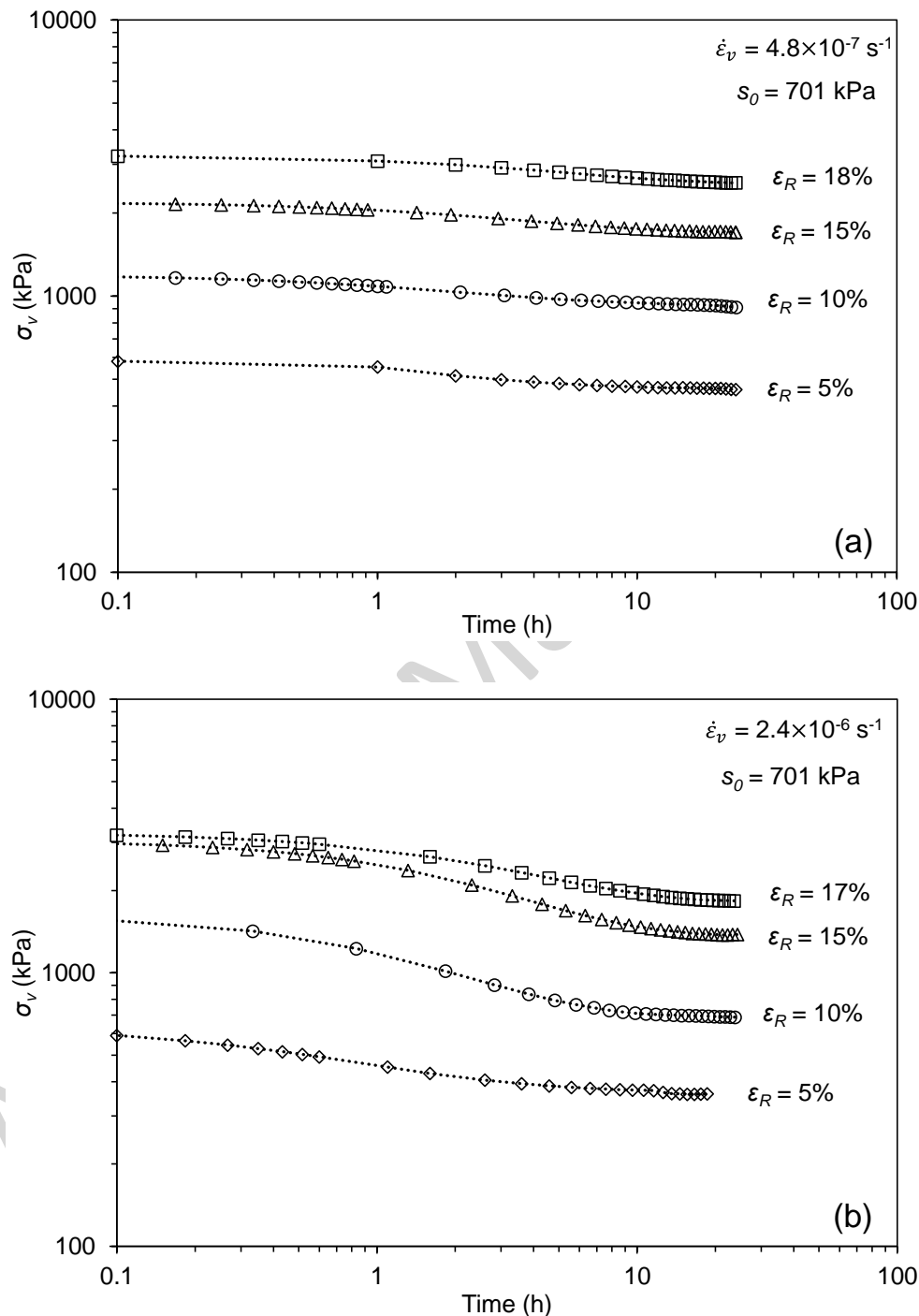
284

285

286 **Fig. 9.** Variation of  $\sigma_v$  and  $\Delta u$  with time during MS-CRS tests: (a) MCRSru33-A; (b) MCRSru33-B

287 Fig. 10 presents the variations of relaxed stresses with time in a log-log scale. Higher stress-  
288 relaxation rates are observed for higher pre-relaxation strains. Furthermore, an approximately  
289 linear relationship between the vertical total stress and time is observed during relaxation stage

290 and after dissipation of  $u_{exc}$ . Similar results have been reported in the literature for saturated  
291 soft clays (e.g. Yin and Graham 1989; Kim and Leroueil 2001; Yin et al. 2014).



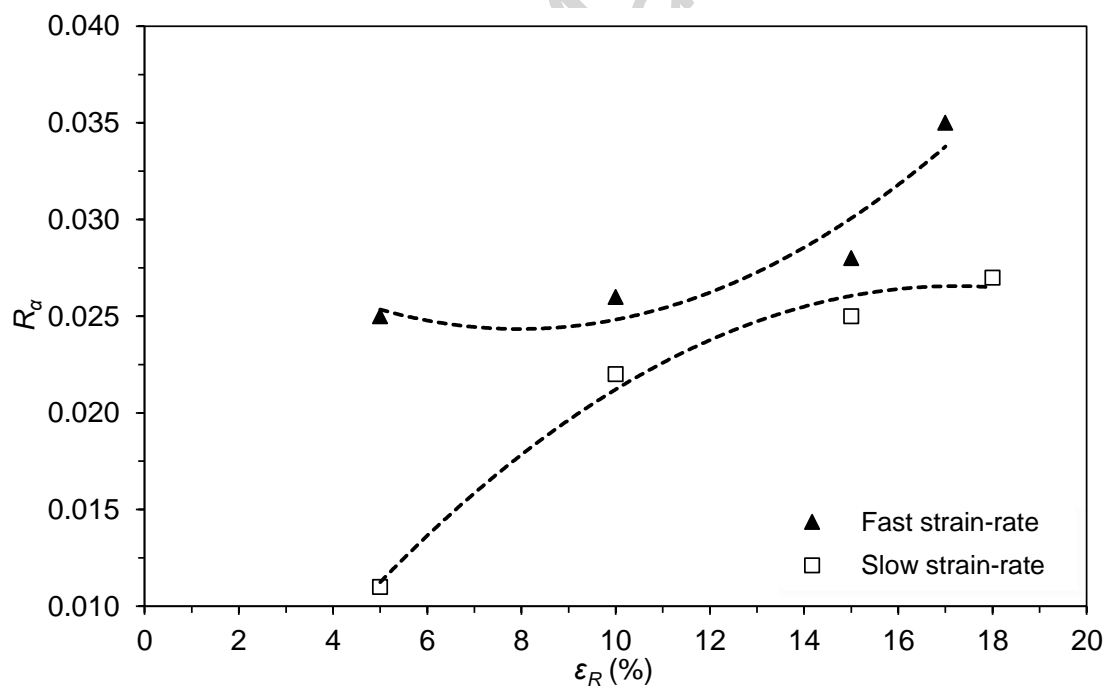
293

294 **Fig. 10.** Relaxation of stresses with time at different pre-relaxation strain levels in log-log scale for

295

strain-rates of: (a)  $4.8 \times 10^{-7} \text{ s}^{-1}$ ; (b)  $2.4 \times 10^{-6} \text{ s}^{-1}$

296 As shown in Table 5, with change in  $\varepsilon_R$ , values of  $R_\alpha$  vary within the ranges of 0.011 – 0.027  
297 and 0.025 – 0.035 respectively for slow and fast pre-relaxation strain-rates (Fig. 11), indicating  
298 dependency of the relaxation coefficient to the pre-relaxation strain (or stress) and strain-rate.  
299 The observed ranges of  $R_\alpha$  for the 24 hours relaxation stages of MS-CRS tests are, however,  
300 higher than the ranges obtained from SS-CRS tests with minimum of 210 hours relaxation  
301 duration. In essence, the higher calculated  $R_\alpha$  values for MS-CRS tests appear to correspond to  
302 the decelerating relaxation phase, characterised with higher relaxation rate, whereas the  $R_\alpha$   
303 values for SS-CRS tests correspond to the residual relaxation phase, characterised with lower  
304 relaxation rate. Larger relaxation periods are, therefore, required for better estimation of  
305 relaxation coefficient, and hence, more accurate determination of time-dependent parameters  
306 based on  $R_\alpha = C_\alpha/C_c$  relationship.



307

308

**Fig. 11.** Variation of  $R_\alpha$  with pre-relaxation strain level and pre-relaxation strain-rate



309 **Conclusion**

310 Results of a set of SS-CRS and MS-CRS oedometer tests performed on reconstituted London  
311 Clay specimens under saturated and unsaturated conditions and varied strain-rates were  
312 presented. From the test data, the following conclusions can be drawn;

- 313 1) Increase in strain-rate results in an increase in  $\sigma_p$  and decrease in  $C_c$  values. Similar  
314 effects were also observed with increase in suction.
- 315 2) Compression curves from CRS tests exhibit higher  $\sigma_p$  than the MSL tests. Moreover, at  
316 a given void ratio, the higher the strain-rate the higher would be the vertical stress.
- 317 3) At a constant suction, the higher the strain-rate, the higher the  $\sigma_p$ . Similarly, at a constant  
318 strain-rate, the higher the suction, the higher the  $\sigma_p$ .
- 319 4) Increase in  $\sigma_p$  with suction appears to follow an approximately linear trend for fast,  
320 slow, and oedometeric strain-rates.
- 321 5) The process of stress-relaxation consists of three phases; (1) fast relaxation, (2)  
322 decelerating relaxation, and (3) residual relaxation.
- 323 6) At a constant pre-relaxation stress ( $\sigma_0$ ), increase in suction results in a decrease in the  
324 rate of stress-relaxation during fast and decelerating relaxation phases, as well as in the  
325 magnitude of the overall relaxed stresses ( $\Delta\sigma$ ).
- 326 7) At a constant suction, the higher the pre-relaxation strain-rate, the higher would be the  
327 rate and magnitude of the relaxed stresses.
- 328 8) The  $R_\alpha = C_\alpha/C_c$ , suggested by Yin et al. (2014) for saturated soft clays, was observed,  
329 with an approximation, to also be valid for unsaturated reconstituted specimens in the  
330 range of applied vertical stresses and soil suctions in this study.
- 331 9) A higher rate and magnitude of relaxed stresses were observed with increase in pre-  
332 relaxation strains (and consequently pre-relaxation stresses).

- 333 10) At a constant strain level and suction, an increase in the  $\Delta\sigma$  values by a factor of 2.2 –  
334 3.6 was observed with an increase in the pre-relaxation strain-rate by a factor of 5. At  
335 the same strain level, increase in pre-relaxation strain-rate also results in an increase in  
336  $R_\alpha$  values under constant suction.
- 337 11) More test results over a wider range of suctions and strain-rates are required for  
338 adequately characterisation of the pre-relaxation strain-rate effect on the stress-  
339 relaxation process in unsaturated clays.

## 340 Notations

341 *The following symbols are used in this paper:*

$e$	=	void ratio
$e_0$	=	initial void ratio
$s$	=	soil suction
$s_0$	=	initial suction
$t$	=	time
$t_R$	=	relaxation duration
$u_a$	=	pore-air pressure
$u_{exc}$	=	excess pore-water pressure
$u_w$	=	pore-water pressure
$w$	=	gravimetric water content
$w_0$	=	initial gravimetric water content
$w_L$	=	liquid limit
$w_P$	=	plastic limit
$C_c$	=	compression index
$C_r$	=	reloading index
$C_s$	=	swelling index
$C_\alpha$	=	creep index
$D$	=	particle diameter
$G_s$	=	specific gravity
$I_p$	=	plasticity index
$R_\alpha$	=	coefficient of stress-relaxation
$\alpha$	=	represents the ratio $C_\alpha/C_c$
$\varepsilon_a$	=	axial strain
$\varepsilon_R$	=	pre-relaxation strain
$\dot{\varepsilon}_v$	=	strain-rate

- $\sigma_0$  = pre-relaxation total vertical stress
- $\sigma_p$  = yield vertical net stress
- $\sigma_v$  = applied vertical total stress
- $\sigma_s$  = residual total vertical stress
- $\sigma'_v$  = vertical effective stress
- $\sigma_{vm}$  = maximum applied vertical stress
- $\sigma_{vnet}$  = vertical net stress
- $\sigma_{pCRS}$  = yield vertical net stress obtained from CRS tests
- $\sigma_{pMSL}$  = yield vertical net stress obtained from MSL tests
- $\Delta\sigma$  = relaxed stress
- $\Delta u$  = change in pore-water pressure
- $\zeta$  = residual stress ratio
- AEV = air-entry value
- HCT = high-capacity tensiometer
- LC = London clay
- MSL = multi-staged loading
- NCL = normal compression line
- SSL = single-staged loading
- CRS = constant rate of strain
- 1D = one-dimensional
- PPR = pore-water ratio

Accepted Manuscript

343 **References**

- 344 ASTM-D4186-06. 2006. "Standard test method for one-dimensional consolidation properties  
345 of saturated cohesive soils using controlled-strain loading." West Conshohoken, PA:  
346 ASTM International.
- 347 Bagheri, M. 2018. "Experimental investigation of the time- and rate-dependent behaviour of  
348 unsaturated clays." PhD Thesis, University of Nottingham, UK.
- 349 Bagheri, M., M. Mousavi Nezhad and M. Rezaia. 2019. "A CRS oedometer cell for  
350 unsaturated and non-isothermal tests." *Geotech. Test. J.* 43 (forthcoming).  
351 <https://doi.org/10.1520/GTJ20180204>.
- 352 Bagheri, M., M. Rezaia and M. Mousavi Nezhad. 2015. "An experimental study of the initial  
353 volumetric strain rate effect on the creep behaviour of reconstituted clays." In IOP Conf.  
354 Series: Earth and Environmental Science. 26(1): 012034, IOP Publishing.
- 355 Bagheri, M., M. Rezaia and M. Mousavi Nezhad. 2018. "Cavitation in high-capacity  
356 tensiometers: effect of water reservoir surface roughness." *Geotech. Research.* 5(2):  
357 81-95. <https://doi.org/10.1680/jgere.17.00016>.
- 358 Borja, R.I. 1992. "Generalized creep and stress relaxation model for clays." *J. Geotech. Eng.*  
359 118( 11): 1765-1786. [https://doi.org/10.1061/\(ASCE\)0733-9410\(1992\)118:11\(1765\)](https://doi.org/10.1061/(ASCE)0733-9410(1992)118:11(1765)).
- 360 Cheng, C.M. and J.H. Yin. 2005. "Strain-rate dependent stress-strain behavior of undisturbed  
361 Hong Kong marine deposits under oedometric and triaxial stress states." *Marine*  
362 *Geores. Geotech.* 23(1-2): 61-92. <https://doi.org/10.1080/10641190590953818>.
- 363 Hanzawa, H., T. Fukaya and K. Suzuki. 1990. "Evaluation of engineering properties for an  
364 Ariake clay." *Soils Found.* 30(4): 11-24. [https://doi.org/10.3208/sandf1972.30.4\\_11](https://doi.org/10.3208/sandf1972.30.4_11).
- 365 Karstunen, M., M. Rezaia, N. Sivasithamparam, M. Leoni and Z.-Y Yin. 2010. "Recent  
366 developments on modelling time-dependent behaviour of soft natural clays." In Proc.,

- 367 XXV Mexican National Meeting of Soil Mechanics and Geotechnical Engineering,  
368 Acapulco, Mexico, pp. 931-938.
- 369 Khoshghalb, A. and N. Khalili. 2013. "A meshfree method for fully coupled analysis of flow  
370 and deformation in unsaturated porous media." *Int. J. Numeric. Anal. Methods*  
371 *Geomech.* 37(7): 716-743. <https://doi.org/10.1002/nag.1120>.
- 372 Khoshghalb, A., A.Y. Pasha and N. Khalili. 2015. "A fractal model for volume change  
373 dependency of the water retention curve." *Géotechnique* 62(2): 141-146.  
374 <https://doi.org/10.1680/geot.14.T.016>.
- 375 Kim, Y. T. and S. Leroueil. 2001. "Modeling the viscoplastic behavior of clays during  
376 consolidation: application to Berthierville clay in both laboratory and field conditions."  
377 *Can. Geotech. J.* 38(3): 484-497. <https://doi.org/10.1139/t00-108>.
- 378 Ladanyi, B. and M.B. Benyamina. 1995. "Triaxial relaxation testing of a frozen sand." *Can.*  
379 *Geotech. J.* 32(3): 496-511. <https://doi.org/10.1139/t95-052>.
- 380 Lai, X., S. Wang, H. Qin and X. Liu. 2010. "Unsaturated creep tests and empirical models for  
381 sliding zone soils of Qianjiangping landslide in the Three Gorges." *J. Rock Mech.*  
382 *Geotech. Eng.* 2(2): 149-154. <https://doi.org/10.3724/SP.J.1235.2010.00149>.
- 383 Leroueil, S., D. Perret and J. Locat. 1996. "Strain rate and structuring effects on compressibility  
384 of a young clay." In: Proc., Measuring and Modelling of Time Dependent Soil  
385 Behavior, Geotechnical Special Publication, edited by T.C. Sheahan and V.N.  
386 Kaliakin, 137-150. Reston.
- 387 Leroueil, S., F. Tavenas, L. Samson and P. Morin. 1983. "Preconsolidation pressure of  
388 Champlain clays. Part II. Laboratory determination." *Can. Geotech. J.* 20(4): 803-816.  
389 <https://doi.org/10.1139/t83-084>.

- 390 Nash, D.F.T., G.C. Sills and L.R. Davison. 1992. "One-dimensional consolidation testing of  
391 soft clay from Bothkennar." *Géotechnique* 42(2): 241-256.  
392 <https://doi.org/10.1680/geot.1992.42.2.241>.
- 393 Nazer, N.S.M. and A. Tarantino. 2016. "Creep response in shear of clayey geo-materials under  
394 saturated and unsaturated conditions." E-UNSAT 2016, E3S Web of Conferences 9:  
395 14023. <https://doi.org/10.1051/e3sconf/20160914023>.
- 396 Qiao, Y., A. Ferrari, L. Laloui and W. Ding. 2016. "Nonstationary flow surface theory for  
397 modeling the viscoplastic behaviors of soils." *Comp. Geotech.* 76: 105-119.  
398 <https://doi.org/10.1016/j.compgeo.2016.02.015>.
- 399 Rezania, M., M. Bagheri, M. Mousavi Nezhad and N. Sivasithamparam. 2017a. "Creep  
400 analysis of an earth embankment on a soft soil deposit with and without PVD  
401 improvement." *Geotext. Geomemb.* 45(5): 537-547.  
402 <https://doi.org/10.1016/j.geotexmem.2017.07.004>.
- 403 Rezania, M., M. Mousavi Nezhad, H. Zanganeh, J. Castro and N. Sivasithamparam. 2017b.  
404 "Modeling pile setup in natural clay deposit considering soil anisotropy, structure, and  
405 creep effects: case study." *Int. J. Geomech.* 17(3): 04016075.  
406 [https://doi.org/10.1061/\(ASCE\)GM.1943-5622.0000774](https://doi.org/10.1061/(ASCE)GM.1943-5622.0000774).
- 407 Sorensen, K.K. 2006. "Influence of viscosity and ageing on the behaviour of clays." Ph.D.  
408 Thesis, University College London.
- 409 Sorensen, K.K., B.A. Baudet and B.Simpson. 2010. "Influence of strain rate and acceleration  
410 on the behaviour of reconstituted clays at small strains." *Géotechnique*. 60(10): 751-  
411 761. <https://doi.org/10.1680/geot.07.D.147>.
- 412 Tong, F. and J.H. Yin. 2013. "Experimental and constitutive modeling of relaxation behaviors  
413 of three clayey soils." *J. Geotech. Geoenv. Eng.* 139(11): 1973-1981.  
414 [https://doi.org/10.1061/\(ASCE\)GT.1943-5606.0000926](https://doi.org/10.1061/(ASCE)GT.1943-5606.0000926).

- 415 Wang, M., X. Xu, J. Li, F. Shen and Y. Li. 2017. "An experiment study on stress relaxation of  
416 unsaturated lime-treated expansive clay." *Env. Earth Sci.* 76: 241.  
417 <https://doi.org/10.1007/s12665-017-6562-4>.
- 418 Yin, J.H. and J. Graham. 1989. "Viscous-elastic-plastic modelling of one-dimensional time  
419 dependent behaviour of clays." *Can. Geotech. J.* 26(2): 199-209.  
420 <https://doi.org/10.1139/t89-029>.
- 421 Yin, Z.Y. and P.Y. Hicher. 2008. "Identifying parameters controlling soil delayed behaviour  
422 from laboratory and in situ pressuremeter testing." *Int. J. Numer. Analy. Methods*  
423 *Geomech.* 32(12): 1515-1535. <https://doi.org/10.1002/nag.684>.
- 424 Yin, Z.Y., Q.Y. Zhu, J.H. Yin and Q. Ni. 2014. "Stress relaxation coefficient and formulation  
425 for soft soils." *Géotechnique Letters.* 4(1): 45-51.  
426 <https://doi.org/10.1680/geolett.13.00070>.
- 427 Zhou, A.N., D. Sheng, S.W. Sloan and A. Gens. 2012. "Interpretation of unsaturated soil  
428 behaviour in the stress-saturation space, I: Volume change and water retention  
429 behaviour." *Comp. Geotech.* 43: 178-187.  
430 <https://doi.org/10.1016/j.compgeo.2012.04.010>.
- 431